MEASUREMENTS AND MODELING OF SNOW ENERGY BALANCE AND SUBLIMATION FROM SNOW

David G. Tarboton
Utah Water Research Laboratory,
Utah State University,
Logan, Utah 84322-8200
Telephone: 801-797-3172; Fax: 801-797-3663; email: dtarb@cc.usu.edu

Abstract

Snow melt runoff is an important factor in runoff generation for most Utah rivers and a large contributer to Utah's water supply and periodically flooding. The melting of snow is driven by fluxes of energy into the snow during warm periods. These consist of radiant energy from the sun and atmosphere, sensible and latent heat transfers due to turbulent energy exchanges at the snow surface and a relatively small ground flux from below. The turbulent energy exchanges are also responsible for sublimation from the snow surface, particularly in arid environments, and result in a loss of snow water equivalent available for melt. The cooling of the snowpack resulting from sublimation also delays the formation of melt runoff. This paper describes measurements and mathematical modeling done to quantify the sublimation from snow. Measurements were made at the Utah State University drainage and evapotranspiration research farm. I attempted to measure sublimation directly using weighing lysimeters. Energy balance components were measured, by measuring incoming and reflected radiation, wind, temperature and humidity gradients.

An energy balance snowmelt model was tested against these measurements. The model uses a lumped representation of the snowpack with two state variables, namely, water equivalent and energy content relative to a reference state of water in the solid phase at $0^{o}C$. This energy content is used to determine snowpack average temperature or liquid fraction. The model is driven by inputs of air temperature, precipitation, wind speed, humidity and solar radiation. The model uses physically based calculations of radiative, sensible, latent and advective heat exchanges. An equilibrium parameterization of snow surface temperature accounts for differences between snow surface temperature and average snowpack temperature without having to introduce additional state variables. This is achieved by incorporating the snow surface thermal conductance, which with respect to heat flux is equivalent to stomatal and aerodynamic conductances used to calculate evapotranspiration from vegetation. Melt outflow is a function of the liquid fraction, using Darcy's law. This allows the model to account for continued melt outflow even when the energy balance is negative.

The purpose of the measurements presented here was to test the sublimation and turbulent exchange parameterizations in the model. However the weighing lysimeters used to measure sublimation suffered from temperature sensitive oscillations that mask short term sublimation measurements. I have therefore used the measured data to test the models capability to represent the overall seasonal accumulation and ablation of snow.

Description of Experiment

The experiment reported here was conducted at the USU drainage and evapotranspiration research farm in Cache Valley. Instrumentation in place is designed for the study of evapotranspiration from agricultural lands, but for this study was utilized for the study of winter snow cover. The instrumentation consisted of two 1 m^2 weighing lysimeters and meteorological and energy balance equipment. The weighing lysimeters are 1 x 1 x 1 m metal boxes embedded flush with the surface and filled with soil, vegetated with grass similar to the surrounding agricultural field. Load cells (underneath in the case of one lysimeter and at the corners for the other) record the weight of soil, grass, soil moisture and snow over the 1 m^2 area. Meltwater infiltrates into the lysimeter so does not result in a weight change. Changes in weight are due only to addition or removal of mass from the surface, which in the case of snow can be due to precipitation, condensation, sublimation and wind drifting.

Meteorological and energy balance instrumentation used is listed in table 1.

Table 1: Meteorological Instrumentation

2 Net Radiometers (Fritchen type Q6 and Q4) installed 1m above the snow surface.
2 Lycor pyranometers that record solar radiation. One was pointed down to estimate albedo.
1 Eppley pyranometer to record incident solar radiation.
2 Everest Interscience model 4000 Infrared surface temperature sensors.
4 Anemometers at heights 0.6, 0.9, 1.4 and 2.4 m above the ground surface.
4 Viasala temperature and relative humidity sensors at height 0.58, 0.90, 1.44, 2.57 m above the ground surface.
2 REBS Ground heat flux plates
Thermocouple ladder. This consisted of 14 copper/constantine thermocouples at the following levels: -0.075, -0.025, 0, 0.05, 0.125, 0.2, 0.275, 0.35, 0.425, 0.5, 0.575, 0.65, 0.725, 0.8 m, from the ground surface. The first two thermocouples were buried and the third placed on the ground. The remainder were suspended on fishing line strung between two upright posts.
Heated (unshielded) tipping bucket rain/snow gage.
Wind direction sensor

Two campbell scientific 21X dataloggers powered by a deep cycle 12 volt battery charged by a solar panel were used to take measurement readings every minute and record 30 minute averages for output.

The dataloggers were downloaded during biweekly visits at which time the sensors were also inspected and cleared of snow and grime buildup. During these visits, snow depth and water

equivalent was measured at eight locations using an Adirondack snow tube sampler. To guard against the danger of bridging in the snow between snow over the lysimeters and surrounding snow which would distort the weights and inferred sublimation a plastic batten and saw was used to saw the snow between the lysimeter and surrounding. This was done from a ladder supported between two trestles over the lysimeter so as not to disturb the snow on or near the lysimeter. This procedure was only partly successful as we did notice some abrupt changes in lysimeter weight that coincided with the sawing. We also found that the lysimeter weight measurements had a diurnal temperature sensitivity that precluded using them for short term sublimation measurements. They still provide an overall measurement of snow accumulation.

The USU drainage and irrigation experimental farm is located in Cache Valley near Logan, Utah, USA (41.6° N, 111.6° W, 1350m elevation). The weather station and instrumentation are in a small fenced enclosure at the center of a large open field. There are no obstructions to wind in any direction for at least 500m. Cache valley is a flat bottomed enclosed valley surrounded by mountains that reach elevations of 3000m. During winter periods of settled weather strong temperature inversions accompanied by very cold (-20 °C) nighttime temperatures and night and morning fog develop. Unsettled stormy periods serve to break the inversion. During the period of this experiment the ground was snow covered from November 20, 1992 to March 22, 1993. Air temperatures ranged from -23 °C to 16 °C and there was 190 mm of precipitation (mostly snow, but some rain). The snow accumulated to a maximum depth of 0.5 m with maximum water equivalent of 0.14 m. Table 2 gives a chronology of the events and measurements. The instrumentation was only fully functional for the latter half of the winter, which will be the focus of the analysis.

Table 2. Chronology.

From	To	Day	Event
11/20/92		-41	First snowfall 6 mm.
11/20/92	1/13/93	-41 to 13	Several snowstorms resulting in an accumulation of 86 mm of water equivalent and depth of 400 mm.
1/13/93		13	*Supplementary equipment (thermocouple ladder and air temperature and humidity profile) is finally functional.*
1/17/93		17 to 19	*Datalogger battery failure, some data lost.*
1/18/93	1/25/93	18 to 25	Period of unsettled weather (12 mm precipitation).
1/25/93		25	*Heated precipitation gage and downward pointing pyranometer installed and functional.*
1/26/93	2/8/93	26 to 39	Inversion and fog.
2/8/93	2/25/93	39 to 56	Period of unsettled weather (45 mm precipitation).
2/26/93	3/9/93	57 to 68	Inversion and fog.
3/10/93	3/11/93	69 to 70	Rain and snow (20 mm precipitation). Highest water equivalent accumulation of 139 mm was recorded just prior to this event which initiated melt.
3/11/93	3/14/93	70 to 73	Clear warm weather. Melt continues.
3/15/93	3/16/93	74 to 75	Light rain (2 mm).
3/17/93	3/18/93	76 to 77	Heavy rain (18.5 mm) that caused considerable snowmelt.
3/19/93	3/22/93	78 to 81	Remaining snow melted rapidly.

Energy Balance Snowmelt Model

The energy balance model used (Chowdhury et al., 1992; Bowles et al., 1992; Bowles et al., 1994; Tarboton et al., 1995) was developed for purposes of erosion prediction and water balance modeling. The snowpack is characterized by two primary state variables, water equivalent, W [m], and energy content, U, [kJ/m^2]. The state variable, energy content U, is defined relative to a reference state of water at 0°C in the ice (solid) phase. U greater than zero means the snowpack (if any) is isothermal with some liquid content and U less then zero can be used to calculate the snowpack average temperature, T, [°C]. Energy content is defined as the energy content of the snowpack plus a top layer of soil with depth D_e [m]. This provides a simple buffering against numerical instabilities when the snowpack is shallow, as well as simple approximations of frozen ground and melting of snow falling on warm ground. We discuss below the choice of D_e and the role it plays in the model.

The model is designed to be driven by inputs of air temperature, T_a [°C]; wind speed, V [m/s]; relative humidity, RH; precipitation, P [m/hr]; incoming solar Q_{si} and longwave Q_{li} radiation [kJ/m^2/hr]; and ground heat flux Q_g [kJ/m^2/hr] (taken as 0 when not known) at each time step. When incoming solar radiation is not available it is estimated as extra terrestrial radiation (from sun angle) times an atmospheric transmission factor, Tr, estimated from the daily temperature range using the procedure given by Bristow and Campbell (1984). When incoming longwave radiation is not available it is estimated based on air temperature, the Stefan-Boltzman equation and a parameterization of air emissivity due to Satterlund (1979) adjusted for cloudiness using Tr.

Given the state variables U and W, their evolution in time is determined by solving energy and mass balance equations.

$$\frac{dU}{dt} = Q_{sn} + Q_{li} + Q_p + Q_g - Q_{le} + Q_h + Q_e - Q_m \quad (1)$$

$$\frac{dW}{dt} = P_r + P_s - M_r - E \quad (2)$$

In the energy balance equation terms are (all in kJ/m^2/hr): Q_{sn}, net shortwave radiation; Q_{li}, incoming longwave radiation; Q_p, advected heat from precipitation; Q_g, ground heat flux; Q_{le}, outgoing longwave radiation; Q_h, sensible heat flux; Q_e, latent heat flux due to sublimation/condensation; Q_m, advected heat removed by meltwater. In the mass balance equation (all in m/hr of water equivalent) terms are: P_r, rainfall rate; P_s snowfall rate; M_r, meltwater outflow from the snowpack; E, sublimation from the snowpack. Many of these fluxes depend functionally on the state and input driving variables. We elaborate on the parameterization of these functional dependencies below. Equations (1) and (2) form a coupled set of first order, nonlinear

ordinary differential equations. They can be summarized in vector notation as:

$$\frac{d\underline{X}}{dt} = \underline{F}(\underline{X}, \text{driving variables}) \tag{3}$$

where $\underline{X} = (U, W)$ is a state vector describing the snowpack. With $\underline{X}$ specified initially, this is an initial value problem. A large variety of numerical techniques are available for solution of initial value problems of this form. Here we have adopted a Euler predictor-corrector approach (Gerald, 1978).

$$\underline{X}' = \underline{X}_i + \Delta t\, \underline{F}(\underline{X}_i, \text{driving variables}) \tag{4}$$

$$\underline{X}_{i+1} = \underline{X}_i + \Delta t \frac{\underline{F}(\underline{X}_i, \text{driving variables}) + \underline{F}(\underline{X}', \text{driving variables})}{2} \tag{5}$$

where Δt is the time step, $\underline{X}_i$ refers to the state at time t_i and $\underline{X}_{i+1}$ refers to the state at time $t_{i+1}=t_i+\Delta t$. This is a second order finite difference approximation, with global error proportional to Δt^2 (Gerald, 1978, p257).

Parameterization

Depth averaged temperature - T: The snow and interacting soil layer average temperatures are obtained from the energy content and water equivalent, relative to 0°C ice phase.

If $U < 0$	$T = U/(\rho_w W C_s + \rho_g D_e C_g)$	All solid phase	(6)
If $0 < U < \rho_w W h_f$	$T = 0°C.$	Solid and liquid mixture	(7)
If $U > \rho_w W h_f$	$T = \dfrac{U - \rho_w W h_f}{\rho_g D_e C_g + \rho_w W C_w}$	All liquid	(8)

In the above the heat required to melt all the snow water equivalent is $\rho_w W h_f$ [kJ] where h_f is the heat of fusion [333.5 kJ kg^{-1}] and U in relation to this determines the solid-liquid phase mixtures. The heat capacity of the snow is $\rho_w W C_s$ [kJ/°C] where ρ_w is the density of water [1000 kg m^{-3}] and C_s the specific heat of ice [2.09 kJ kg^{-1} $°C^{-1}$]. The heat capacity of the soil layer is $\rho_g D_e C_g$ [kJ/°C] where ρ_g is the soil density [≈1700 kg m^{-3}] and C_g the specific heat of soil [≈2.1 kJ kg^{-1} $°C^{-1}$]. These together determine T when $U < 0$. In practice, unless we allow ponded water (which we don't) W will always be 0 in (8). The heat capacity of liquid water, $\rho_w W C_w$, where C_w is the specific heat of water [4.18 kJ kg^{-1} $°C^{-1}$], is however retained in (8) for numerical

consistency during time steps when the snowpack completely melts.

Heat flow in snow and soil is governed by Laplace's equation. The depth of penetration of changes in surface temperature can be evaluated from the expression (Rosenberg, 1974):

$$\frac{R_z}{R_s} = \exp\left(- z \left(\frac{\pi}{\alpha P} \right)^{\frac{1}{2}} \right) \tag{9}$$

where R_s is the range of temperature oscillation at the surface, R_z the range of temperature oscillation at depth z, P the period of oscillation, and α the thermal conductivity. For soil α is typically in the range 0.004 to 0.006 cm^2/s. Figure 1 shows R_z/R_s versus z for $\alpha = 0.005$ cm^2/s for various periods. This shows that for oscillations less than one week the effect at 40 cm is damped to less than 30% and even for monthly oscillations is still damped 50% at 40 cm depth. This suggests using $D_e = 40$ cm in our model. Rosenberg (1974) also suggests this as an effective depth. The state variable U represents energy content above this level. The ground heat flux represents heat transport at this depth and is therefore a long term average. Diurnal oscillating ground heat fluxes above this depth are absorbed into U, the energy stored in the snow and soil above depth D_e.

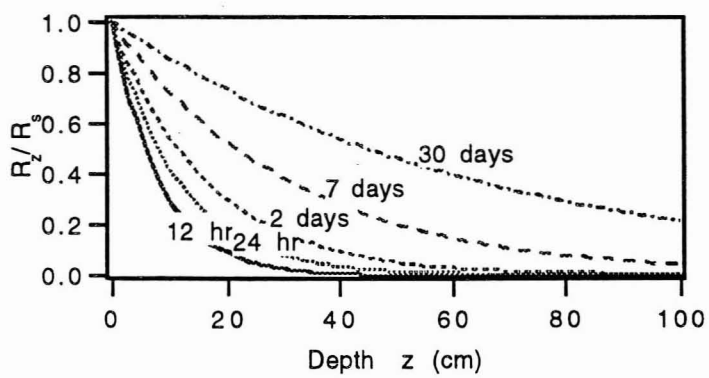

Figure 1. Depth of penetration of temperature fluctuations into soil with $\alpha = 0.005$ cm^2/s.

Net Shortwave Radiation, Q_{sn}: This is calculated as

$$Q_{sn} = Q_{si}\,(1\text{-}A) \tag{10}$$

where Albedo, A, is calculated based on the age of the snow surface using a parameterization described by Dickinson et al. (1993). For shallow snowpacks (depth less than 0.1 m) the albedo is interpolated between the bare ground value (0.25) and snow value.

Outgoing Longwave Radiation, Q_{le}: Snow is essentially a black body, with emissivity $\varepsilon_s \approx 0.99$. Outgoing radiation is

$$Q_{le} = \varepsilon_s \sigma \left(T_s^{abs} \right)^4 \tag{11}$$

where σ is the Stefan Boltzmann constant [2.07×10^{-7} kJ m^{-2} hr^{-1} K^{-4}] and the superscript "abs" in T_s^{abs} indicates that this is absolute temperature [K].

Snow fall accumulation and heat with precipitation: Measured precipitation rate, P, is partitioned into rain, P_r, and snow, P_s, (both in terms of water equivalent depth) using the following rule based on air temperature, T_a, (U.S. Army Corps of Engineers, 1956)

$$\begin{aligned} P_r &= P && T_a \geq T_r = 3\ ^oC \\ P_r &= P(T_a - T_b)/(T_r - T_b) && T_b < T_a < T_r \\ P_r &= 0 && T_a \leq T_b = -1\ ^oC \\ P_s &= P - P_r \end{aligned} \tag{12}$$

where T_r is a threshold air temperature above which all precipitation is rain and T_b a threshold air temperature below which all precipitation is snow.

The temperature of rain is taken as the greater of the air temperature and freezing point and the temperature of snow the lesser of air temperature and freezing point. The advected heat is the energy required to convert this precipitation to the reference state (0°C ice phase).

$$Q_p = P_s C_s \rho_w \min(T_a, 0\ ^\circ C) + P_r \left[h_f \rho_w + C_w \rho_w \max(T_a, 0\ ^\circ C) \right] \tag{13}$$

Turbulent fluxes, Q_h, Q_e, E: Sensible and latent heat fluxes between the snow surface and air above are modeled using the concept of flux proportional to temperature and vapor pressure gradients with constants of proportionality, the so called turbulent transfer coefficients or diffusivity a function of windspeed and surface roughness. Considering a unit volume of air, the heat content is $\rho_a C_p T_a$ and the vapor content $\rho_a q$, where ρ_a is air density (determined from atmospheric pressure and temperature), C_p air specific heat capacity [1.005 kJ kg^{-1} $^oC^{-1}$], and q specific humidity [kg water vapor per kg air]. Heat transport towards the surface, Q_h [kJ/m^2/hr] is given by:

$$Q_h = K_h \rho_a C_p \left(T_a - T_s \right) \tag{14}$$

where K_h is heat conductance [m/hr] and T_s is the snow surface temperature. Vapor transport

away from the surface (sublimation), M_e [kg/hr] is:

$$M_e = K_e \rho_a (q_s - q) \tag{15}$$

where q_s is the surface specific humidity and K_e the vapor conductance [m/hr].

By comparison with the usual expressions for turbulent transfer in a logarithmic boundary layer profile (Male and Gray, 1981; Anderson, 1976; Brutsaert, 1982; Calder, 1990) for neutral condition, one obtains the following expression:

$$K_h = K_e = \frac{k^2 V}{\left[\ln (z/z_0)\right]^2} = K \tag{16}$$

where V is wind speed [m/hr] at height z [m]; z_0 is roughness height at which the logarithmic boundary layer profile predicts zero velocity [m]; and k is von Karman's constant [0.4]. The subscript n denotes that these are conductances in neutral conditions. Recognizing that the latent heat flux towards the snow is:

$$Q_e = -h_v M_e \tag{17}$$

and using the relationship between specific humidity and vapor pressure and the ideal gas law one obtains:

$$Q_e = K_e \frac{h_v\, 0.622}{R_d\, T_a^{abs}} \left(e_a - e_s(T_s)\right) \tag{18}$$

where e_s is the vapor pressure at the snow surface snow, assumed saturated at T_s, and calculated using a polynomial approximation (Lowe, 1977); e_a is air vapor pressure, R_d is the dry gas constant [287 J kg^{-1} K^{-1}] and h_v the latent heat of sublimation [2834 kJ/kg]. The water equivalent depth of sublimation is:

$$E = -\frac{Q_e}{\rho_w h_v} \tag{19}$$

When there is a temperature gradient near the surface, buoyancy effects may enhance or dampen the turbulent transfers. This can be quantified in terms of the Richardson number or Monin-Obukhov length. We had hoped that the lysimeter measurements made here would have provided

data to allow us to determine the effect of stability on snow sublimation. However since that did not work out the results presented here use neutral buoyancy.

Snow Surface Temperature, T_s: Since snow is a relatively good insulator, T_s is in general different from T. This is accounted for using an equilibrium approach that balances energy fluxes at the snow surface. Heat conduction into the snow is calculated using the temperature gradient and thermal diffusivity of snow, approximated by:

$$Q = \kappa \rho_s C_s (T_s - T)/Z_e = K_s \rho_s C_s (T_s - T) \tag{20}$$

where κ is snow thermal diffusivity [m^2 hr^{-1}] and Z_e [m] an effective depth over which this thermal gradient acts. The ratio κ/Z_e is denoted K_s and termed snow surface conductance analogous to the heat and vapor conductances. A value of K_s is obtained by assuming a depth, Z_e equal to the depth of penetration of a diurnal temperature fluctuation calculated from equation (9) (Rosenberg, 1974). Z_e is chosen so that R_z/R_s is small. In fact K_s is used as a tuning parameter, with this calculation used to define a reasonable range. Then assuming equilibrium at the surface, the surface energy balance gives.

$$Q = Q_{sn} + Q_{li} + Q_h(T_s) + Q_e(T_s) + Q_p - Q_{le}(T_s) \tag{21}$$

where the dependence of Q_h, Q_e, and Q_{le} on T_s is through equations (14), (18) and (11).

Analogous to the derivation of the Penman equation for evaporation the functions of T_s in this energy balance equation are linearized about a reference temperature, T* and the equation is solved for T_s:

$$T_s^{abs} = \frac{Q_{sn}+Q_{li}+Q_p+KT_a^{abs}\rho_a C_p - 0.622 K h_v \rho_a \left(e_s(T^*) - e_a - T^{*abs}\Delta \right)/P_a + 3\varepsilon_s \sigma T^{*abs^4} + \rho_s C_s T^{abs} K_s}{\rho_s C_s K_s + K \rho_a C_p + 0.622 \Delta K h_v \rho_a / P_a + 4 \varepsilon_s \sigma T^{*abs^3}} \tag{22}$$

where $\Delta = de_s/dT$. This equation is used in an iterative procedure with an initial estimate $T^* = T_a$, in each iteration replacing T* by the latest T_s. The procedure converges to a final T_s which if less than freezing is used to calculate surface energy fluxes. If the final T_s is greater than freezing it means that the energy input to the snow surface cannot be balanced by thermal conduction into the snow. Surface melt will occur and the infiltration of meltwater will account for the energy difference and T_s is then set to 0°C.

Meltwater Outflux, M_r and Q_m: The energy content state variable U determines the liquid content of the snowpack. This, together with Darcy's law for flow through porous media, is used to determine the outflow rate.

$$M_r = K_{sat} S^{*3} \tag{23}$$

where K_{sat} is the snow saturated hydraulic conductivity [≈160 m hr^{-1}] and S* is the relative saturation in excess of water retained by capillary forces. This expression is based on Male and Gray (1981 p400 eqn 9.45). S* is given by:

$$S^* = \frac{\text{liquid water volume - capillary retention}}{\text{pore volume - capillary retention}} = \left(\frac{L_f}{1 - L_f} - L_c \right) / \left(\frac{\rho_w}{\rho_s} - \frac{\rho_w}{\rho_i} - L_c \right) \tag{24}$$

where $L_f = U/(\rho_w h_f W)$ denotes the mass fraction of total snowpack (liquid and ice) that is liquid, L_c [0.05] the capillary retention as a fraction of the solid matrix water equivalent, and ρ_i the density of ice [917 kg m^{-3}].

This melt outflow is assumed to be at 0°C so the heat advected with it, relative to the solid reference state is:

$$Q_m = \rho_w h_f M_r \tag{25}$$

Model parameters

Apart from known physical constants and readily estimable quantities the model has adjustable parameters listed in Table 3. The values used were taken from previous work with the model calibrated against data collected at the Central Sierra Snow Laboratory. These results therefore present an independent check of the model in a different setting.

Table 3. Adjustable parameter values

Parameter	Notation	Value
Surface aerodynamic roughness	z_0	0.002 m
Surface conductance	K_S	0.015 m/hr
Snow density	ρ_S	450 kg m^{-3}
Saturated hydraulic conductivity	K_{sat}	160 m/hr
Capillary retention fraction	L_C	0.05

Results and Discussion

Figure 2 gives the measured lysimeter weights, measured snow water equivalent and accumulated precipitation. The measured snow water equivalent values shown are the average from the 8 snow core measurements made each visit. The individual water equivalent measurements usually varied within a range of 10 to 20% from this average. This shows general agreement between weight accumulation on the lysimeters, snow accumulation and precipitation. Figure 3 compares model and measured snow water equivalent for the model run from day 26 to the end of melt. Two model runs are shown, one with the model driven by measured net radiation and the other with the model driven by incoming solar radiation. The first run bypasses the albedo and outgoing longwave radiation calculations so serves only to test the models sensible and latent heat flux components. The second run is a more realistic check on overall model performance. For both runs the model was initialized with the measured day 26 water equivalent of 0.104 m and energy content based on the average temperature of thermocouples in the snow and soil. This energy content was, -1136 kJ/m^2. These results show that the model does reasonably well at representing snow accumulation and melt. The second model run, with solar radiation as the primary energy input, was used for the remainder of the comparisons in this paper.

Figure 4. shows modeled and measured snow (and soil) energy content. The measured energy content was estimated from the measured water equivalent (linearly interpolated between measurements) and snow and soil temperatures averaged from the thermocouple ladder measurements. There is obviously a large discrepancy between modeled and measured energy content early on, and given this it is surprising how well the model does at representing other aspects of the snow accumulation and melt processes. The lowest energy content on day 39 would predict an average snow and soil temperature of -14 °C. This is well below the observed snow temperatures shown on figure 5. These discrepancies indicate that the model loses too much energy during cold periods, suggesting that the snow surface conductance may be too large. It also indicates that temperature fluctuations do not penetrate to the full interacting soil layer depth, D_e [0.4 m] suggesting that perhaps D_e should be reduced. After day 70 (March 20) the model energy content is above zero due to the liquid water content of the snow. This is the melt period. The measured energy, estimated from thermocouple measurements of snow and soil temperatures, does not account for liquid water in the snow.

Figures 6a-f present detailed results for the period from January 26 to February 7 (day 26 to 38) during which there was a strong temperature inversion and no measurable precipitation, although there was condensation and accumulation of frozen fog. During this period the snow depth was 0.4 m. The sensor heights are given with respect to the ground so the lowest vapor pressure and temperature sensors were only 0.2 m above the snow surface. The lysimeters (only lysimeter 2 is shown in fig 6a, but lysimeter 1 was similar) recorded a diurnal oscillation in weight that is I believe an effect of the cold temperatures on the electronics or load cell system. The oscillations which correlate well with air temperature amount to 2 mm of water equivalent. Based on net radiation measurements the net radiation could only supply energy to sublimate a maximum

of 0.6 mm/day (if all energy goes to sublimation) in this period. The oscillations therefore mask any sublimation signal and preclude the use of these lysimeter measurements for the study of short term sublimation. Figure 6b shows the model water equivalent on an expanded scale where you can see that it does go through a very small diurnal oscillation (up to 0.1 mm/day) with nighttime condensation and daytime sublimation. This oscillation is out of phase with the vapor pressure measurements which increase during the day then drop at night. This suggests a recycling process where the snow surface layer is sublimated during the day then redeposited during nighttime cooling. There is a net accumulation from day 32 to day 33 when the vapor pressures (figure 6d) are high. Then on day 34 there is a period of relatively strong wind (figure 6c) and low vapor pressure (figure 6d) that results in a relatively large modeled sublimation and drop in water equivalent (figure 6b). Gradients in vapor pressure (the difference between the lines on figure 6d) coincide with modeled condensation and sublimation periods (figure 6b). Figure 6f compares model and measured infrared snow surface temperatures. This indicates that the equilibrium procedure for calculation of snow surface temperature works reasonably well.

Detailed results for the melt period (March 19, day 69 to March 23, day 82) are shown in figures 7a-h. The onset of melt was triggered by the 20 mm of precipitation, rain and snow mix on day 69 and 70. Following the precipitation strong winds and low humidity (vapor pressure, figure 7g) induces sublimation in the model over days 71 and 72 (figure 7h). There is some suggestion of a downward trend (implying sublimation) in the lysimeter trace on figure 7a. With this sublimation and cooler air temperatures there is minimal melt modeled on days 71 and 72. Freezing of the snow surface is well modeled as indicated by the model and measured snow surface temperatures (figure 7f). Warmer weather and higher humidity from day 73 on are characterized by positive sensible heat (higher temperatures at the upper sensor, fig 7e) and condensation (higher vapor pressure at the higher sensor, fig 7g) which both add energy to the snowpack, which consequently melts rapidly. The horizontal dashed line on figure 7g is 6.1 mb, the saturation vapor pressure of water over ice at freezing point. Vapor pressures higher than this imply a downward vapor pressure gradient which will result in condensation. Rain on day 76 makes melting even more rapid. Figure 7a indicates that over the whole season, according to the model, net sublimation was only a small fraction (the difference between the dashed lines) of the snow mass. This was due to the persistent inversions and high humidity associated with valley fog.

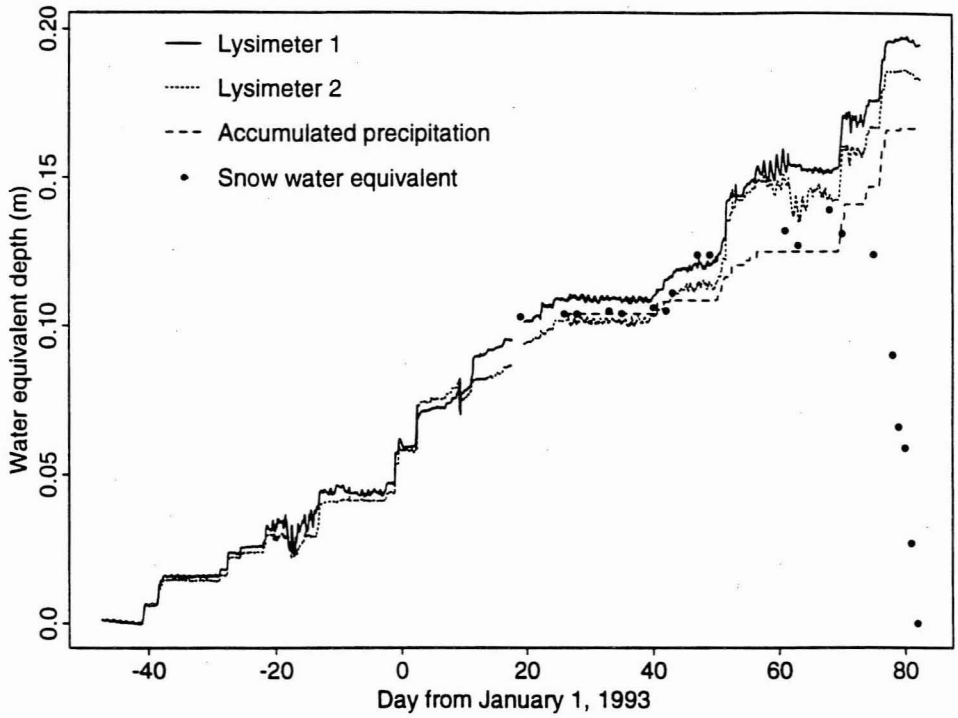

Figure 2. Overall snow accumulation and ablation measurements.

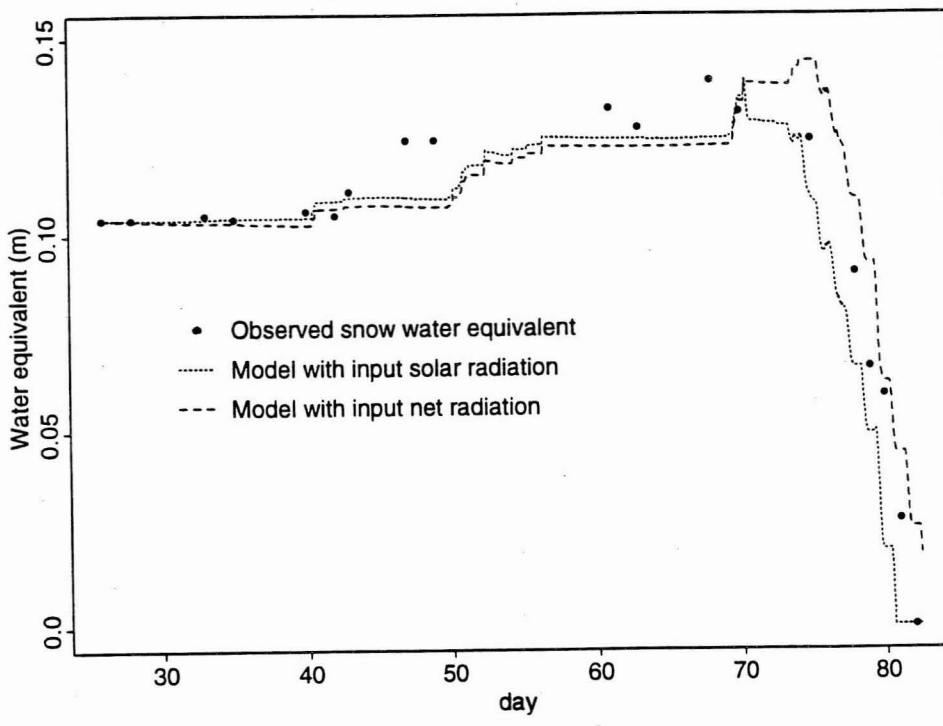

Figure 3. Comparison of observed and modeled snow water equivalent.

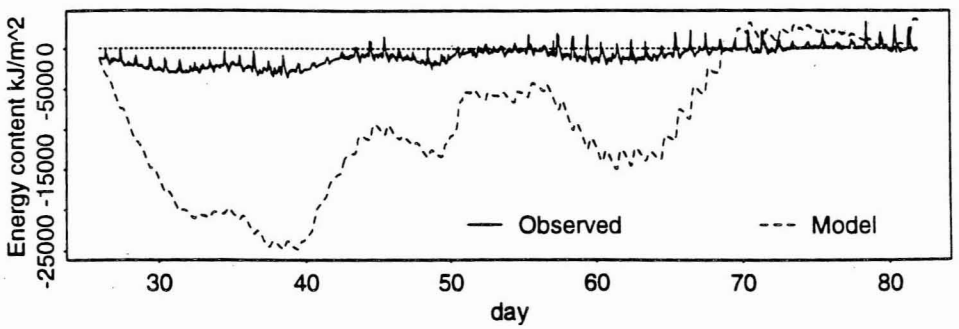

Figure 4. Comparison of measured and modeled energy content of the snow and top 0.4 m of soil.

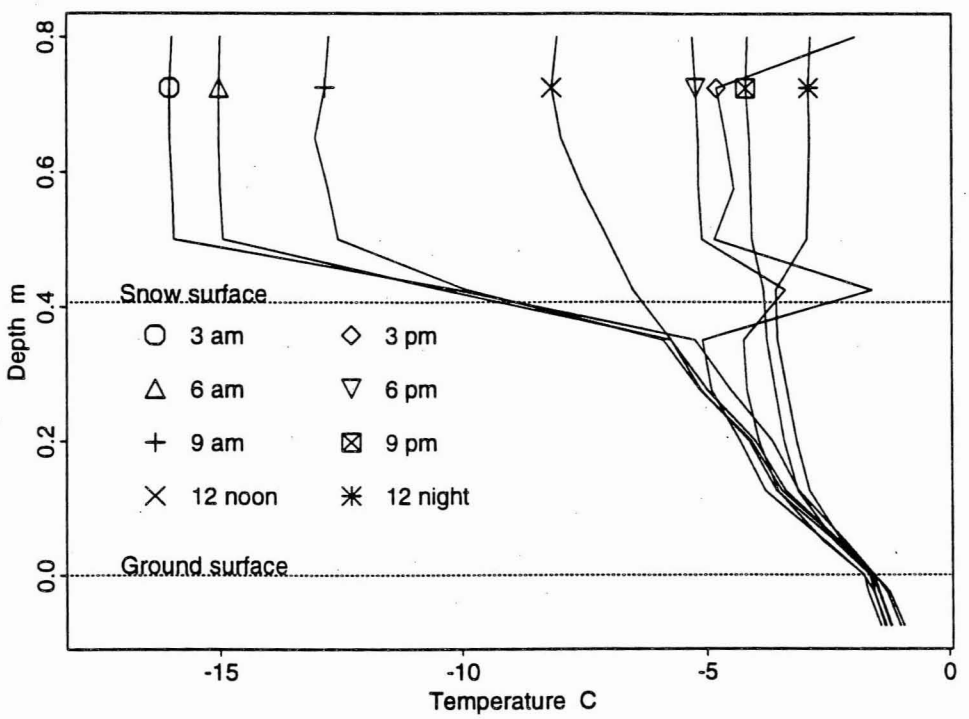

Figure 5. Measured soil and snow temperatures on February 8, 1993 (day 39).

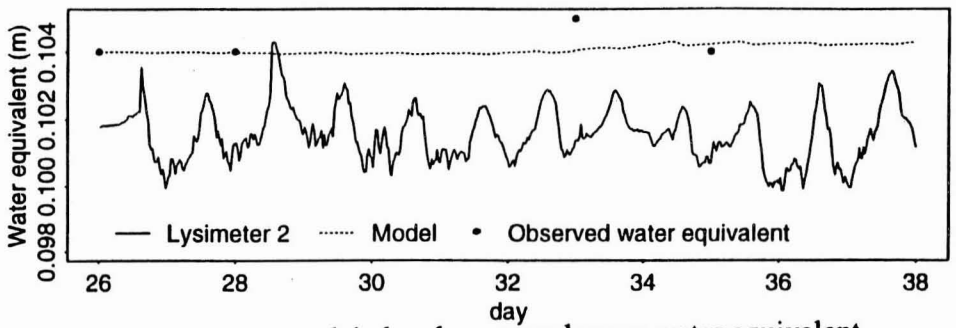

a) Lysimeter, modeled and measured snow water equivalent.

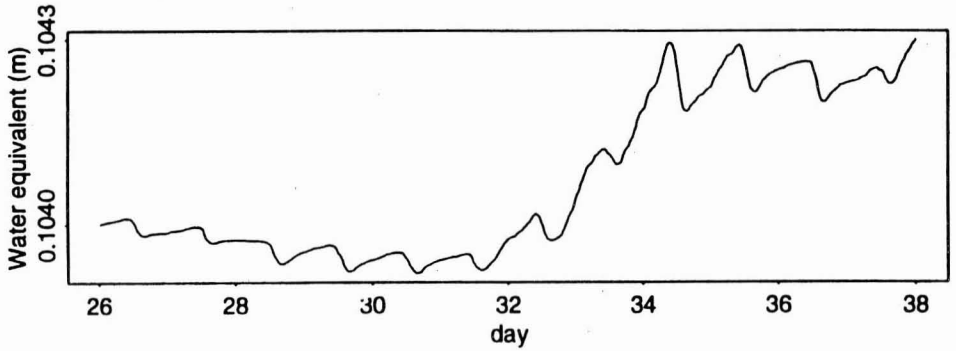

b) Expanded scale model snow water equivalent.

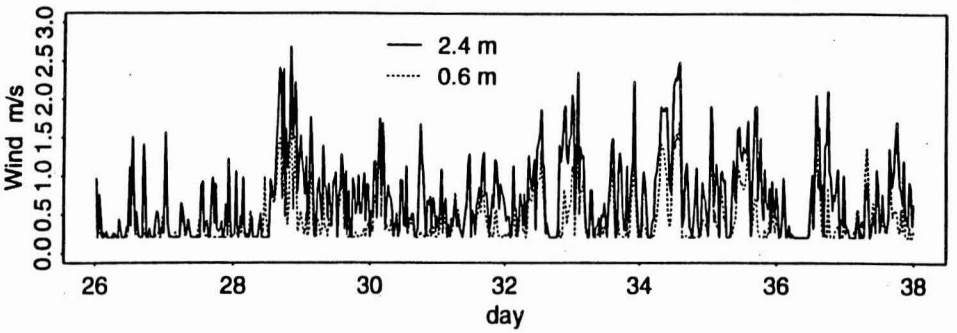

c) Wind velocity at upper and lower levels.

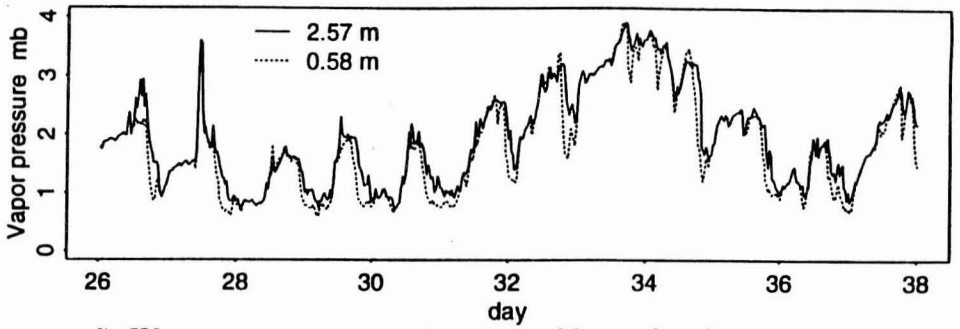

d) Water vapor pressure at upper and lower levels.

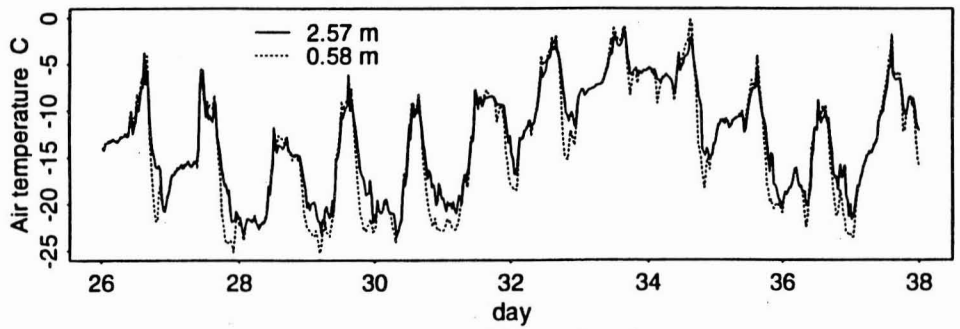

e) Air temperature at upper and lower levels.

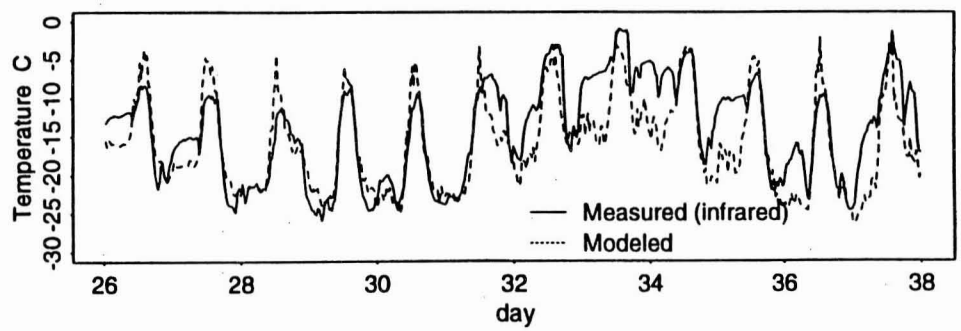

f) Snow surface temperature.

Figure 6. Detailed results for January 16, 1993 to February 7, 1993 (Days 26 to 38).

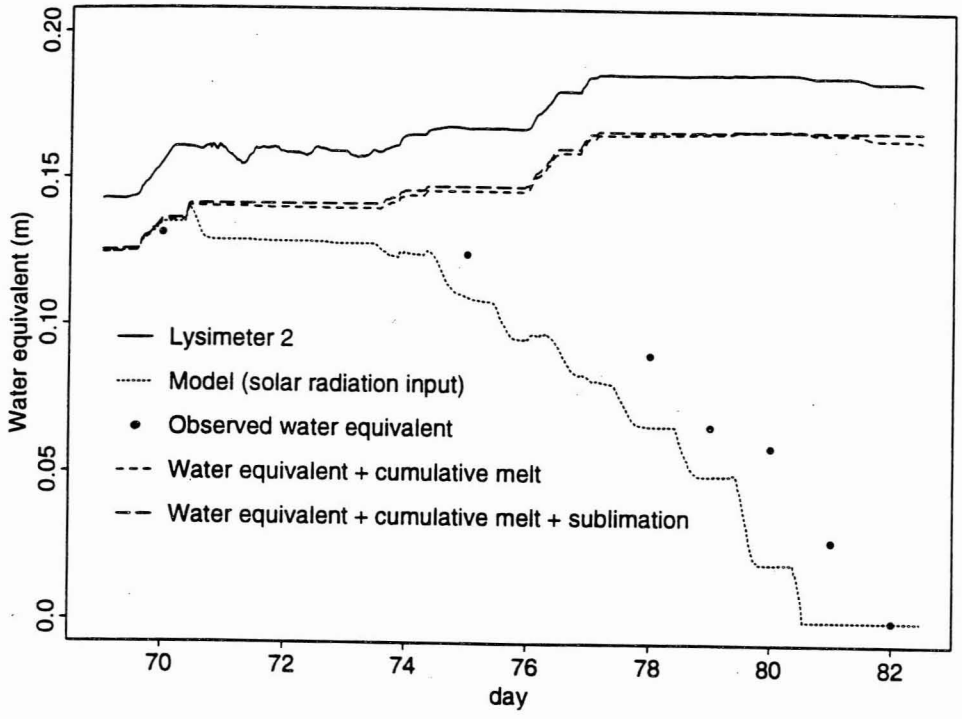

a) Lysimeter, modeled and measured snow water equivalent, accumulated melt and sublimation.

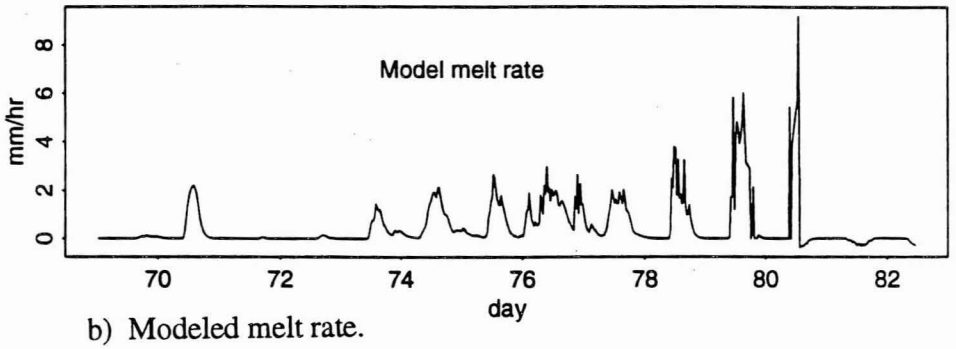

b) Modeled melt rate.

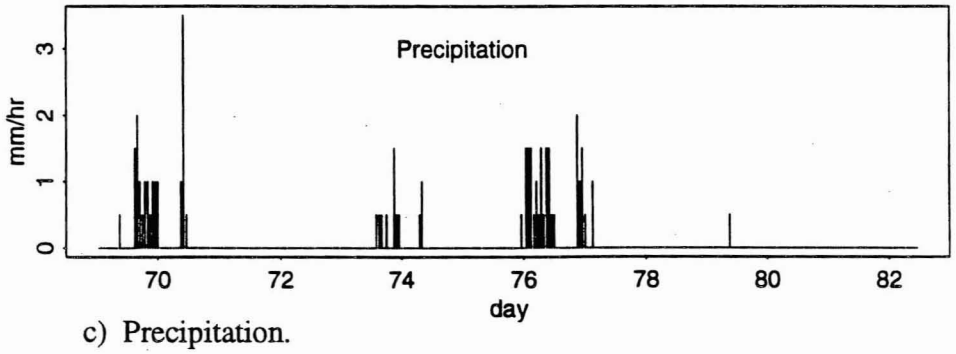

c) Precipitation.

Figure 7. Detailed results for melt period, March 9, 1993 to March 23, 1993 (Days 69 to 82).

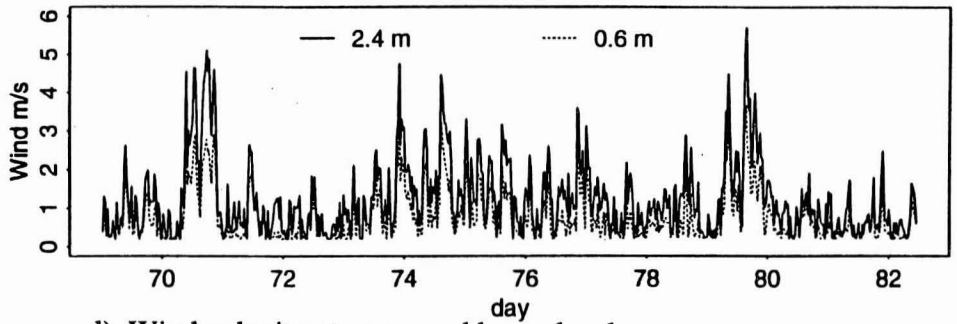

d) Wind velocity at upper and lower levels

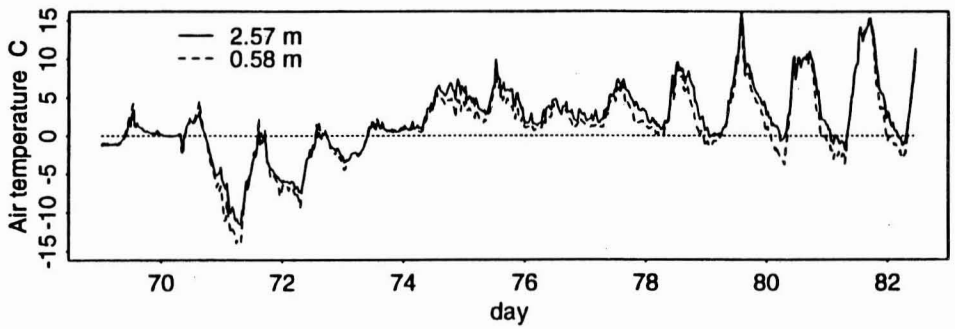

e) Air temperature at upper and lower levels.

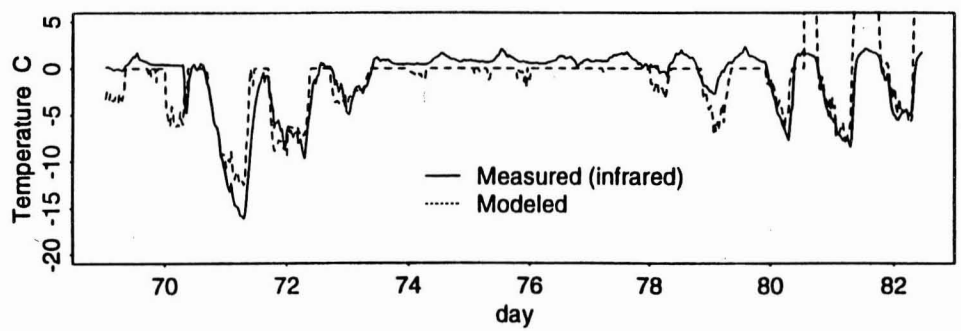

f) Snow surface temperature.

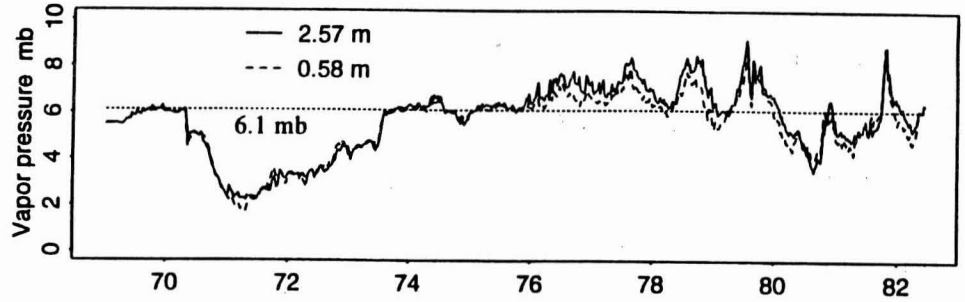

g) Water vapor pressure at upper and lower levels.

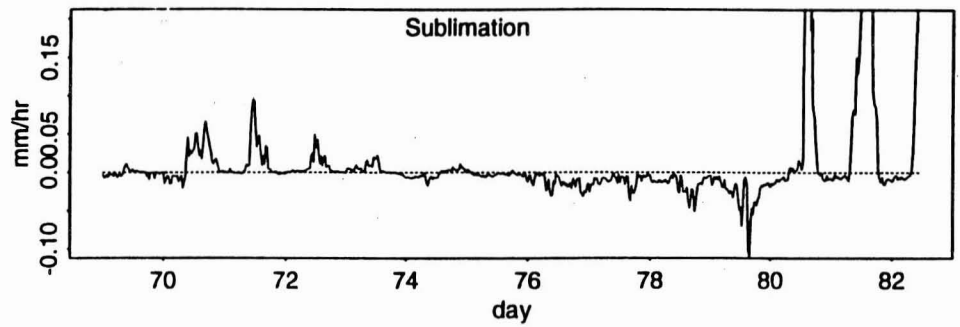

h) Modeled sublimation.

Figure 7. Detailed results for melt period, March 9, 1993 to March 23, 1993 (Days 69 to 82), continued.

Conclusions

An experiment to quantify the sublimation and energy balance of snow was conducted the winter of 1992/93 at the Utah State University drainage and evapotranspiration research farm near Logan, Utah, USA. The experiment was not altogether successful in that large temperature dependent oscillations in the weight recorded by the lysimeters precluded the measurement of sublimation. However the meteorological variables measured were used to test an energy balance snowmelt model. Comparisons against measured snow water equivalent and measured snow surface temperatures indicate satisfactory performance of the model in representing these aspects of the snow accumulation, energy and melt processes. Deficiencies in the models representation of the snow energy content were found and will need to be addressed in future work. Future work with this data set could also attempt to remove the temperature dependence from the lysimeter measurements and obtain estimates of measured sublimation. There is also the information necessary to quantify heat flux, somewhat tenuously, as the residual from net radiation, ground heat flux and changes in energy content of the snow. This could then be compared to temperature gradients and modeled heat flux based on wind. It may also be possible to obtain useful information and learn something about the turbulent transfers of sensible and latent heat fluxes from the analysis of gradient information. This will however be difficult as the air temperature and humidity differences measured were small and approach the resolution limit of the sensors. Overall the improvement of our understanding of turbulent processes over snow will require more study and more precise measurements.

Acknowledgements

This work was supported by a Utah State University faculty research grant and the USDA Forest Service joint venture agreement INT-92660-RJVA. Thank you Richard Allen for access to the USU drainage and evapotranspiration research farm instrumentation, data and tremendous assistance in instrumentation setup and data interpretation. Thank you Arijit Chattopadhyay for your efforts as field assistant.

References

Anderson, E. A., (1976), "A Point Energy and Mass Balance Model of a Snow Cover," NOAA Technical report NWS 19, U.S. Department of Commerce.

Bowles, D. S., G. E. Bingham, U. Lall, D. G. Tarboton, E. Malek, B. Rajagopalan, T. Chowdhury and E. Kluzek, (1992), "Development of Mountain Climate Generator and Snowpack Model for Erosion Predictions in the Western United States using WEPP," Phase IV research completion report submitted to the U.S.D.A. Forest Service Intermountain research station under

joint venture agreement INT-92660-RJVA, Utah Water Research Laboratory.

Bowles, D. S., G. E. Bingham, U. Lall, D. G. Tarboton, B. Rajagopalan, T. Chowdhury and E. Kluzek, (1994), "Development of Mountain Climate Generator and Snowpack Model for Erosion Predictions in the Western United States using WEPP," Research Completion Report for the funding period January 1, 1993 to September 30, 1993 of Phase IV, submitted to the U.S.D.A. Forest Service Intermountain research station under joint venture agreement INT-92660-RJVA, Utah Water Research Laboratory.

Bristow, K. L. and G. S. Campbell, (1984), "On the Relationship Between Incoming Solar Radiation and the Daily Maximum and Minimum Temperature," Agricultural and Forest Meteorology, 31: 159-166.

Brutsaert, W., (1982), Evaporation into the Atmosphere, Kluwer Academic Publishers, 299 p.

Calder, I. R., (1990), Evaporation in the Uplands, John Wiley & Sons, Chichester, 148 p.

Chowdhury, T. G., D. G. Tarboton and D. S. Bowles, (1992), "An Energy Balance Snowmelt Model for Erosion Prediction," Eos Transactions AGU, 73(43): Fall Meeting Suppl., 174.

Dickinson, R. E., A. Henderson-Sellers and P. J. Kennedy, (1993), "Biosphere-Atmosphere Transfer Scheme (BATS) Version 1e as Coupled to the NCAR Community Climate Model," NCAR/TN-387+STR, National Center for Atmospheric Research.

Gerald, C. F., (1978), Applied Numerical Analysis, 2nd Edition, Addison Wesley, Reading, Massachusetts, 518 p.

Lowe, P. R., (1977), "An Approximating Polynomial for the Computation of Saturation Vapour Pressure," Journal of Applied Meteorology, 16: 100-103.

Male, D. H. and D. M. Gray, (1981), "Snowcover Ablation and Runoff," Chapter 9 in Handbook of Snow, Principles, Processes, Management and Use, Edited by D. M. Gray and D. H. Male, Pergammon Press, p.360-436.

Rosenberg, N. J., (1974), Microclimate The Biological Environment, John Wiley & Sons, Inc., 315 p.

Satterlund, D. R., (1979), "An Improved Equation for Estimating Long-wave Radiation From the Atmosphere," Water Resources Research, 15: 1643-1650.

Tarboton, D. G., T. G. Chowdhury and T. H. Jackson, (1995), "A Spatially Distributed Energy Balance Snowmelt Model," Paper in preparation for presentation at IAHS symposium, July 3-14, Boulder Colorado.

U.S. Army Corps of Engineers, (1956), "Snow Hydrology, Summary report of the Snow Investigations," , U.S. Army Corps of Engineers, North Pacific Division, Portland, Oregon.